Sustainable Chemistry and Pharmacy 26 (2022) 100620

Contents lists available at ScienceDirect

Sustainable Chemistry and Pharmacy

journal homepage: www.elsevier.com/locate/scp

Physical, mechanical and thermal properties of metakaolin-fly ash geopolymers

M.A. Gómez-Casero [a], C. De Dios-Arana [a], J.S. Bueno-Rodríguez [a], L. Pérez-Villarejo [b], D. Eliche-Quesada [a,*]

[a] Department of Chemical, Environmental, and Materials Engineering, Higher Polytechnic School of Jaén, University of Jaén, Campus Las Lagunillas s/n, 23071, Jaén, Spain

[b] Department of Chemical, Environmental, and Materials Engineering, Higher Polytechnic School of Linares, University of Jaen, Campus Científico-Tecnológico, Cinturón Sur s/n, 23700, Linares, Jaén, Spain

ARTICLE INFO

Keywords:
Geopolymers
Metakaolin
Coal fly ash
Mechanical properties
Thermal properties

ABSTRACT

Due to the large coal fly ash (FA) production and its obvious environmental impact, alternative uses of this by-product must be researched. A considerable effort is being made worldwide on research concerning the reuse of FA as a source of alternative raw materials to produce new binder materials. One of the most promising building materials are geopolymers or alkali-activated materials (AAM). In this study, FA (25–75 wt %) was used to evaluate the potential of using this waste as a source of aluminosilicates for the synthesis of geopolymers to replace metakaolin (MK) as precursor. MK and FA geopolymers were also synthesized as a control. Sodium hydroxide and sodium silicate were used as alkaline-activator mix (Na_2SiO_3/NaOH ratio: 0.92). The geopolymers synthesized were characterized by Fourier Transform Infrared Spectroscopy (FTIR) X-ray diffraction (XRD) and Scanning Electron Microscopy-Energy Dispersive X-ray spectroscopy (SEM-EDS). The results indicate that control geopolymers, MK and FA geopolymers have similar mechanical and thermal properties. However, the MK-FA blended geopolymers have slightly lower compressive strengths and lower thermal conductivity. The decrease in the properties of the FA and MK-FA blended geopolymers may be due to the high solid/liquid ratio used, since the spherical particles of the FA require less liquid due to their higher workability. However, the obtained geopolymers can be a satisfactory solution for the recovery of waste that results in sustainable construction materials that meet the standard to be used for loadbearing concrete masonry units with insulating properties superior to Portland cement approaching the principles of circular economy.

1. Introduction

It is necessary that solid waste produced on a large scale is recycled if sustainable development is to be achieved. Coal is the most complex and most abundant fossil fuel in the world and it is the main source of energy generation. A clear example of the production of solid waste is coal ash from thermal power plants. Its production amounts to 800 million tonnes per year worldwide (Shi et al., 2020). Between 45 and 55% of the ash is reused, the rest is dumped in ponds or surface deposits (Guo et al., 2021; Elavarasan et al., 2021). Despite these environmental disadvantages, their use is expected to continue to increase due to high demand in developed countries

* Corresponding author.
E-mail address: deliche@ujaen.es (D. Eliche-Quesada).

https://doi.org/10.1016/j.scp.2022.100620
Received 31 October 2021; Received in revised form 18 January 2022; Accepted 26 January 2022
Available online 16 February 2022

(Yang et al., 2019). The thermoelectric plants in Spain generate more than 9.5 million tonnes of wastes per year with only 20% of them are used for different applications (ECOBA, 2021). In addition, coal-fired power plants produced approximately 33 million tonnes of CO_2 in 2016, significantly lower than 48 million tonnes of CO_2 produced in 2015 (Red Eléctrica de España, 2017).

Coal fly shes contain not negligible amounts of some of the most harmful chemical elements for human beings and the environment, such as lead, arsenic, cadmium and chromium. Additionally it is responsible for considerable emissions of nitrogen oxide (NOx) and sulphur dioxide (SO_2) (Qin et al., 2019). Although on the other hand, they have some interesting characteristics that make useful for its use as raw materials in construction materials. Fly ashes due to their pozzolanic activity have been used as a partial replacement of Portland cement (Lanzerstorfer, 2018) especially class F fly ashes with low calcium content. While those with high calcium content or class C fly ashes possess in addition to pozzolanic properties cementitious properties making them suitable for cement preparation (Cavusoglu et al., 2021; Wang et al., 2019). Other uses have been as raw material in brick manufacturing (Elavarasan et al., 2021; Eliche-Quesada et al., 2018), in ceramic tiles (Sokolar and Vodova, 2011), as substitute for kaolinite in cordierite manufacturing (He et al., 2005), in soil amelioration (Pandey and Singh, 2010) due to its contents on some useful nutrients as P, S, K or Mg which are beneficial for the plant growth (Yao et al., 2015), for zeolite synthesis (Querol et al., 2002) and treated for recovery valuable metals like Ge (Font et al., 2005) or Ga (Fan and Gesser, 1996).

Geopolymers is defined as an amorphous-to-semi-crystalline, three-dimensional short-range ordered inorganic aluminosilicate cementitious material having the composition $M_2O{\cdot}mAl_2O_3{\cdot}nSiO_2$, where M is one or more alkali/alkaline earth metals and generally, $m \approx 1$ and $2 \leq n \leq 6$ (Koshy et al., 2019). They are composed of successive SiO_4 and AlO_4 tetrahedra connected through an oxygen-bridged bonding framework, in which positive ions (Na^+, K^+, Li^+, or Ca^{2+}) balance the negative charge of Al^{3+} in IV-fold coordination (Xu and van Deventer, 2003). It is a material that can be synthesized using a variety of silicoaluminate sources, including natural minerals as metakaolin and a wide range of industrial wastes and by-products containing appreciable amounts of silica, alumina as coal fly ash (Sajan et al., 2021) or calcium like slags (Li et al., 2010, Casero- Fuentes et al., 2021) and red mud (He et al., 2012), and requires alkaline activation by a strong base.

Some of the most precursors used is metakaolin (MK) because it is rich in aluminium and easily alkali-activation (Chen et al., 2019). Geopolymers exhibits excellent physical strength, suitable acid resistance, low energy consumption, low-carbon emissions and high-efficiency utilization of industrial by-products than Portland cement (Wang et al., 2020). However, they are difficult to produce by using alkaline activating solutions such as alkaline silicates and hydroxides, which have a high economic and environmental cost due to their high energy demand (temperatures close to 1400 °C) and greenhouse gas emissions (Fawer et al., 1999).

On the other hand, determining the thermal conductivity of geopolymers is an important measure when considering their thermal insulation applications in buildings. Thermal conductivity measures the heat transfer in a material, so a lower thermal conductivity value indicates better insulation of the building with the energy savings this entails (Novais et al., 2016). In general, geopolymers have thermal conductivities more than 50% lower than those of Portland cement materials (Feng et al., 2015; Fongang et al., 2015). Very little research has taken into consideration the thermal conductivity of MK-FA geopolymers.

In this manuscript, it is intended to use coal fly ash in large proportion to reduce the environmental impact, studying substitutions from a minimum of 25 wt% to a maximum of 75 wt% of MK by FA, to evaluate its use as a source of aluminosilicates in the synthesis of blended geopolymers reducing its production cost. As a reference, geopolymers using only MK as precursor or only coal fly ash were synthesized. The alkaline activator used was a solution of sodium hydroxide (NaOH) in a concentration of 10 mol/l and sodium silicate (Na_2SiO_3), using a Na_2SiO_3/NaOH ratio of 0.92. Therefore, this work provides a comprehensive study of the optimization of the maximum fly ash ratio to be incorporated into MK and its effect on compressive strength and thermal conductivity. The joint effect of precursor and residue and the correlation in terms of physical properties, mechanical strength, and thermal conductivity have been elucidated.

2. Materials and methods

2.1. Materials

A series of geopolymer specimens were synthesized using as precursors metakaolin (MK) and coal fly ash (FA). MK was obtained calcining kaolin for 4 h at 700 °C. Kaolin was provided by Caobar S.A., located in Taracena (Spain). Metakaolin was replaced for coal fly ash from Endesa's thermal power plant. This plant is found in Carboneras (Spain). The precursors were sieved to a particle size below 150 μm. The chemical composition of raw materials determined by XRF using a Philips Magix Pro PW-2440, can see in the Table 1. The total content of SiO_2 and Al_2O_3 of the FA and MK was 97.0% and 74.3%, respectively. The content of CaO of FA is (9.77 5) being classified like class "F" fly ash or fly ash with a low calcium according to ASTM C618-12 (ASTM C618-12, 2003).

The diffraction pattern of MK shows quartz as the only crystalline phase, presenting amorphous compounds as indicated by the deviation from the 2 theta baseline between 15° and 30°. The diffraction pattern of the FA is more complex and indicates that the residue is made up of partially vitreous mineral particles and crystalline phases, mainly mullite, quartz and hematite and lesser extent gypsum, calcite and lime (Fig. 1).

Table 1
Chemical composition of raw materials: metakaolin and coal fly ash.

	SiO_2	Al_2O_3	Fe_2O_3	CaO	MgO	MnO	Na_2O	K_2O	TiO_2	P_2O_5	SO_3	LOI
MK	54.0	43.0	0.48	0.10	0.10	<0.01	0.01	0.5	0.24	0.05	–	0.44
FA	50.3	21.0	7.02	9.77	1.57	0.05	–	1.87	0.9	0.4	0.82	2.74

The particle size of the precursors can be observed in Fig. 2. A smaller particle size of MK can be observed with respect to FA. Particle sizes d_{10} of 2.23 μm, d_{50} of 9.579 μm and d_{90} of 87.024 μm for MK and d_{10} of 1.88 μm, d_{50} of 19.87 μm and d_{90} of 89.75 μm for FA. Results of the uniformity coefficient obtained from the granulometric distributions indicate a greater uniformity of FA waste than of the MK precursor, with values of 1.47 and 2.84, respectively.

The alkaline activator solution was a mixing of sodium hydroxide 10 M (NaOH) (52.17 wt %) and sodium silicate (Na_2SiO_3) (47.85 wt %). Sodium hydroxide was supplied by pellets with 98% purity and sodium silicate solution (29.2% SiO_2, 8.9% Na_2O y 61.9% H_2O). The Na_2SiO_3/NaOH ratio was 0.92. Both supplied by Panreac S.A. The activator solution had pH of 14.

2.2. Synthesis of MK-FA geopolymers

Different geopolymer compositions have been prepared. MK, FA and MK-FA (75:25, 50:50 and 75:25 wt ratio) (Fig. 3). The different composition are presented in the Table 2. The raw materials, MK and FA were mixed at a slow speed in the dry state for 5 min using a planetary kneader. The alkaline solution is then added to the mixture for 2 min. Finally, the paste is homogenized for 10 min at fast speed. Mixing time is 17 min in total each specimen. The geopolymeric precursors are poured into cylindrical moulds 35 mm in diameter and 70 mm of height beaten on a shaking table to remove air. Subsequently, pastes are cured in a curing chamber at 60 °C and saturated humidity for 1 day. After the first curing period they are demoulded and left in the air in atmospheric conditions for 7 and 28 days. The precursor/activator or solid/liquid ratio is 0.78. The Si/Al and Na/Al molar ratios increase from 1.45 to 0.74 respectively for the 100MK geopolymers, which employs only MK, to 2.94 and 1.54 respectively for the 100FA geopolymers, when only FA residue is used as raw material. The Na/Si molar ratio remains constant at 0.5.

2.3. Testing and characterization

The geopolymers have been characterized by Fourier Transform Infrared Spectroscopy (FTIR) using a Vertex 70 Bruker equipment. The geopolymers were scanned from 4000 to 400 cm^{-1}. Phase analysis was performed between 10 and 60° 2θ with a step size of 0.02° with an Empyean X-Ray diffraction (XRD) equipment with a PIXcel-3D detector from PANalytical using Cu K radiation (λ = 1.5406 Å) at a voltage of 40 kV and an amperage of 40 mA. The XRD difractograms were analyzed using HighScore software. A JEOL SM 840 model Scanning Electron Microscope was used to image the geopolymer samples.

The bulk density, apparent porosity and water absorption of MK-FA geopolymers were determined according to ASTM 642-13 (ASTM 642-13, 2013).

The compressive strength was determined using a MTS 810 Material Test System machine mechanical Tester with a loading capacity of 100 kN using a loading rate of 0.5 MPa/s according to UNE-EN105-11 (UNE-EN105–11:2000/A1:2007) standard. A TA Instruments-Waters LLC® model FOX 50 heat flow meter was used to determine the thermal conductivity of the specimens after 28 days of curing.

3. Results and discussion

3.1. Bulk density, apparent porosity and water absorption

Data obtained for bulk density after 7 and 28 days of curing are shown in the Fig. 3. A bulk density of 1475 and 1430 kg/m^3 and 1590 and 1426 kg/m^3 was obtained for MK and FA geopolymers at 7 and 28 days of curing, respectively. The bulk density of MK-FA

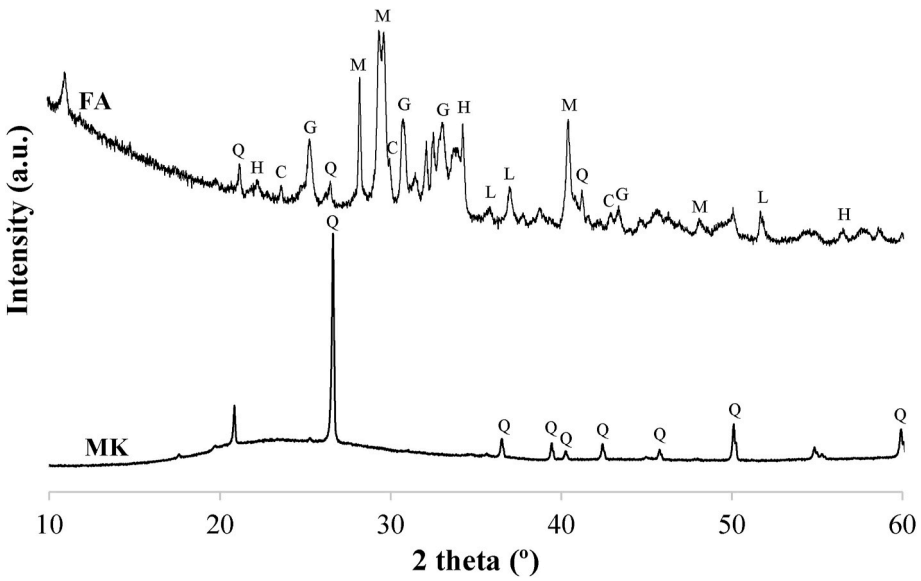

Fig. 1. XRD of precursors: Metakaolin (MK) and coal fly ash (FA). Q: quartz; M: mullite; H: hematite; G: gypsum; C: calcite; L:lime.

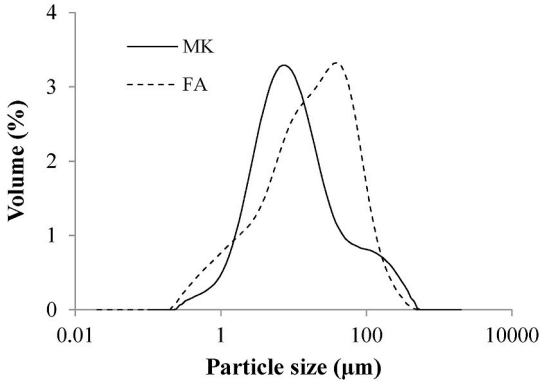

Fig. 2. Particle size distribution of the precursors: metakaolin (MK) and coal fly ash (FA).

blended geopolymers are within 1480–1519 kg/m^3 and 1379–1412 kg/m^3 at 7 and 28 days of curing, respectively. The similarity in the bulk density values may be to the similar relative density of MK (2569 kg/m^3) and FA (2480 kg/m^3). For all geopolymers, a decrease of bulk density was observed with the curing time. Increasing the curing time, the liquid evaporation was greater, leading to greater porosity during the curing process (Rovnaník, 2010). The bulk density of metakaolin geopolymers is reported in the range between 1200 kg/m^3 and 1800 kg/m^3 (Yun-Minga et al., 2016). FA geopolymers present lower bulk densities than those obtained in other studies where bulk densities between 1700 and 2080 kg/m^3 after 28 days of curing are reported (Zulkifly et al., 2021; Cheng-Yong et al., 2017; Aguilar et al., 2010). The apparent porosity and water absorption decreased with the addition of FA at 7 days of curing (Fig. 3). The lowest values of apparent porosity and water absorption of 11.2% and 7.0% at 7 days of curing was found for 100FA, while the highest value 17.7% y 11.7% was for 100MK geopolymers. However, after 28 days of curing, apparent porosity and water absorption increase due to the formation of higher porosity as the FA content increases, presenting values of apparent porosity between 17.9 and 23.7% and water absorption between 11.7 and 13.1%. The porosity also depends on the water trapped in the geopolymer matrix generated during the geopolymerization process (Zulkifly et al., 2021). Excess free water in the geopolymer when exposed to room temperature and low relative humidity results in increased porosity and water absorption. Therefore, although the s/l ratio remains constant in all geopolymers, the different workability of the precursors may affect the quality of consolidation and compaction to a small extent. In addition, the amount of water expelled during the curing process may be slightly different, as well as the amount of water generated and the amount of geopolymer gel formed during the geopolymerization process. The increase in porosity with curing time may be due to excess liquid in the pastes escaping into the environment during the curing process.

3.2. *Compressive strength*

Compressive strength results are shown in the Fig. 4. MK geopolymers have compressive strengths of 21 and 22 MPa at 7 and 28 days of curing, respectively. FA geopolymers have slightly lower values, but close, 18.0 and 18.9 MPa. MK-FA blend geopolymers have lower values that decrease with increasing FA content between 17.5 and 14.4 MPa at 7 days of curing and between 16.0 and 12.9 MPa at 28 days of curing. These results indicate that the FA residue is chemically somewhat less reactive than MK, as indicated by other authors (Cai et al., 2020). All geopolymers except the 25MK-75FA blended geopolymers show compressive strength values after 28 days of curing higher than the minimum value of 13.10 MPa established by the ASTM C90 - 16a (ASTM C90-16a, 2016) standard for loadbearing concrete masonry units. The compressive strength values increase as the Si/Al ratio decreases, except for the FA geopolymers, due to the higher resistance of the aluminosilicate gel with respect to the silicate gel (Fernández-Jiménez et al., 2006). In addition, the Na/Al ratio also influences the compressive strength (Sisol et al., 2019). The compressive strength increases as the Na/Al ratio decreases, except for geopolymer FA, according to other authors (Gingos, 2011). The presence of (C,N)-A-S-H gel in the FA and MK-FA blended geopolymers does not produce an increase in the compressive strength. This may be due to the s/l ratio employed for all the geopolymers synthesized was 0.78. This ratio is the most commonly used ratio for MK (Jaya et al., 2020) with an S/L ratio of 2 being the most commonly used for FA geopolymers (Abdullah, S., et al., 2018). The spherical shape of FA particles provides better workability than plate-like MK particles (Arun et al., 2019). Therefore, FA particles demand less liquid extension due to their higher workability. This excess of forming water can lead to losses in the mechanical properties of FA-MK and FA geopolymers. On the other hand, the lower compressive strength of the MK-FA blended geopolymers could be due to the existence of two types of gels with transition zones of N-A-S-H gel from the reaction of the MK precursor and (N,C)-A-S-H gel containing calcium from the reaction of the FA residue, as indicated by SEM micrographs and EDS analysis (see Fig. 10).

The compressive strength of the MK, FA and MK-FA geopolymers remain practically constant with the curing time, indicating that the Na^+ and OH^- ions are consumed in the initial curing at 60 °C for 1 day and subsequent curing at room temperature for 7 days, so that no new geopolymerization can occur in the samples cured at longer times, by producing the breakage of the Si–O and Al–O bonds of the MK and FA forming sodium aluminosilicate gels. The calcium ions contained in the FA residue interact with the N-A-S-H gel to form (N,C)-A-S-H geopolymerization (Bidwe and Hamane, 2015). Also, the presence of Fe_2O_3 in the precursor fly ash can lead to the formation of ferrosialate gel, which can also strengthen the resulting specimens (Adesanya et al., 2020). Therefore, these geopolymers do not require more than seven days of curing to develop maximum compression resistance. Other authors have also found that the

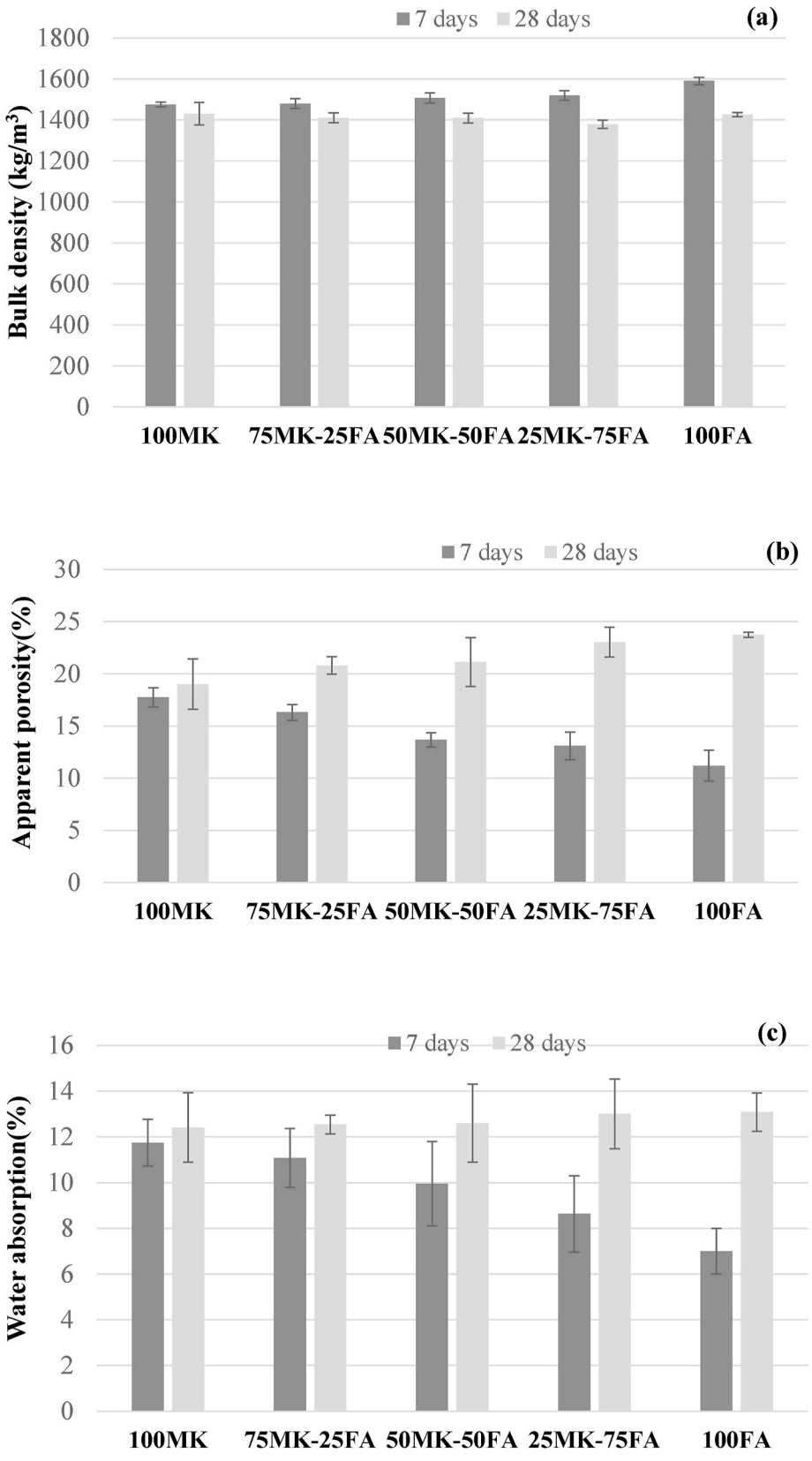

Fig. 3. (a) Bulk density, (b) apparent porosity and (c) water absorption of MK, FA and MK-FA blended geopolymers for 7 and 28 days of curing.

Table 2
Composition of geopolymers synthetized.

Sample	Si/Al Molar ratio	Na/Si Molar ratio	Na/Al molar ratio	MK (g)	FA (g)	Na_2SiO_3 (g)	H_2O (g)	NaOH (g)	M (mol/l)
100MK	1.45	0.51	0.74	450	0	300	195	80	10
75MK-25FA	1.66	0.51	0.86	337.5	112.5	300	195	80	10
50MK-50FA	1.94	0.52	1.02	225	225	300	195	80	10
25MK-75FA	2.34	0.53	1.24	112.5	337.5	300	195	80	10
100FA	2.94	0.53	1.57	0	4500	300	195	80	10

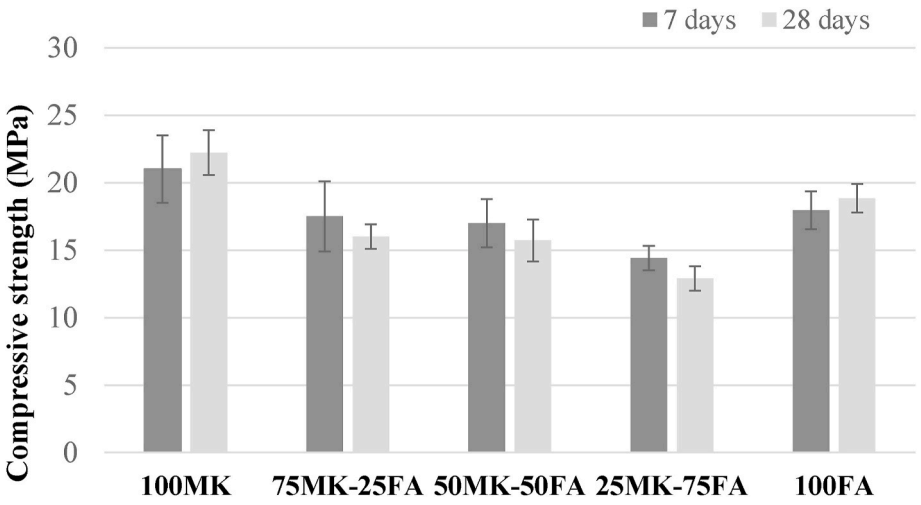

Fig. 4. Compressive strength of MK, FA and MK-FA blended geopolymers at 7 and 28 days of curing.

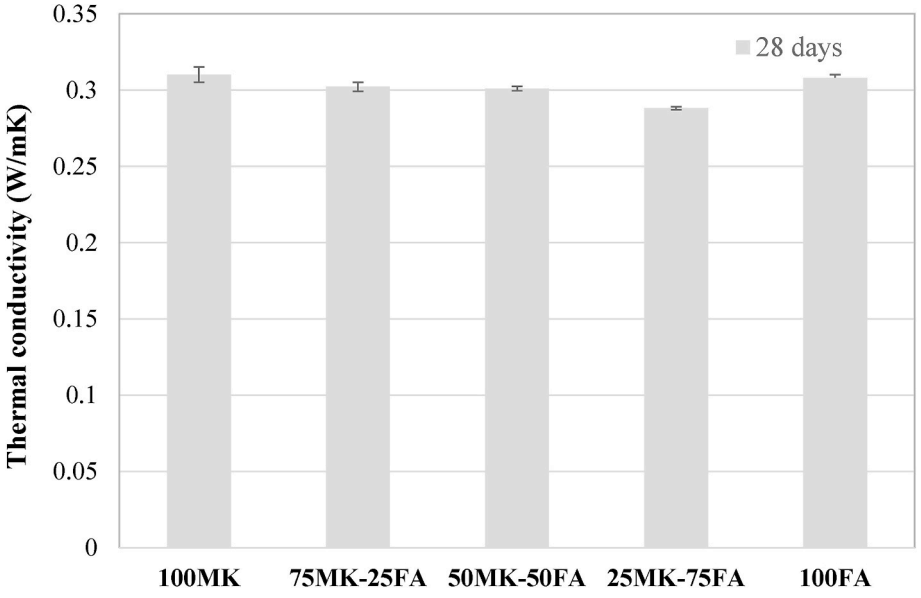

Fig. 5. Thermal conductivity of MK, FA and MK-FA blended geopolymers at 28 days of curing.

first 12 h of curing are crucial for the development of a hard geopolymer structure and the formation could be almost complete 24 h after geopolymerization begins. Thermal curing accelerates the geopolymerization reaction by converting the 2D geopolymer chains into a rigid 3D geopolymer structure (Bing-hui et al., 2014).

The compressive strength results of the MK geopolymers are similar to those obtained by other authors using similar synthesis conditions and Si/Al and Na/Si ratios (Ozer and Soyer-Uzun, 2015). However, the compressive strength results of geopolymers using FA and MK-FA blend geopolymers are very different. Thus, Zulkifly et al., 2021, obtain maximum compressive strengths for FA-MK

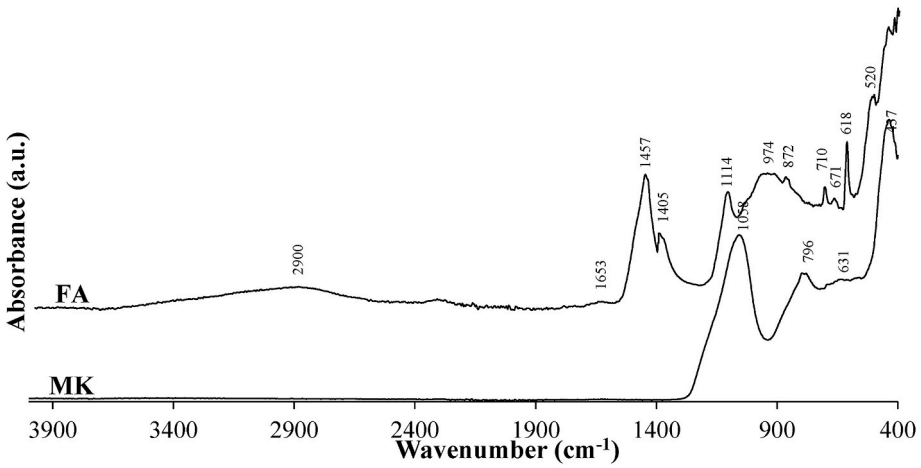

Fig. 6. FTIR spectra of raw materials: metakaolin (MK) and coal fly ash (FA).

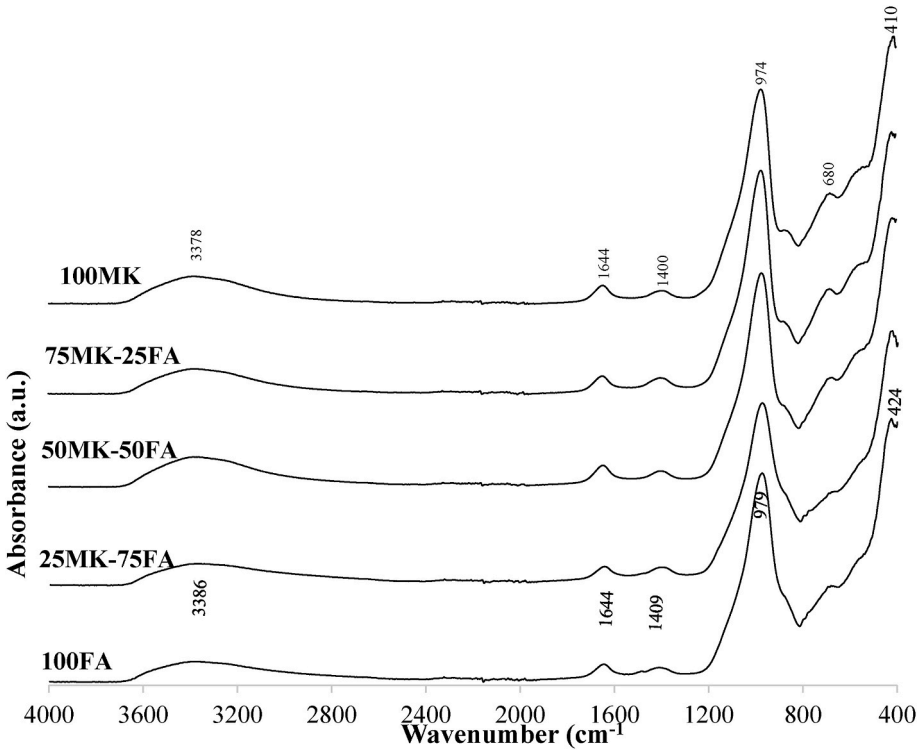

Fig. 7. FTIR spectra of MK, FA and MK-FA blended geopolymers after 7 days of curing.

blend geopolymers of 54.7 MPa after 28 days of curing employing 10 M NaOH, an S/L ratio of 1.2 and a Na_2SiO_3/NaOH ratio of 2.6, obtaining similar values 25 MPa when employing S/L ratios of 0.8. Cai et al. (2020) obtained FA geopolymers with compressive strengths between 3 and 30 MPa as a function of alkali concentration and initial curing temperature. Guo et al. (2021) obtained FA geopolymers with compression strengths of 8.6 MPa, while the addition of 20, 30 and 50 wt% of MK increased the compression strength up to 30 MPa at 7 days of curing.

3.3. Thermal conductivity

The 100MK control geopolymers and 100FA geopolymers have a thermal conductivity of 0.31 W/mK (Fig. 5). The addition of FA to MK produced a decrease in thermal conductivity to 0.29 W/mK for the 25MK-75FA geopolymers following the trend of bulk density and compressive strength. The higher the bulk density and compressive strength, the higher the thermal conductivity value and the lower the insulation capacity. It can be observed that the blended geopolymers show a slightly higher thermal insulation capacity than

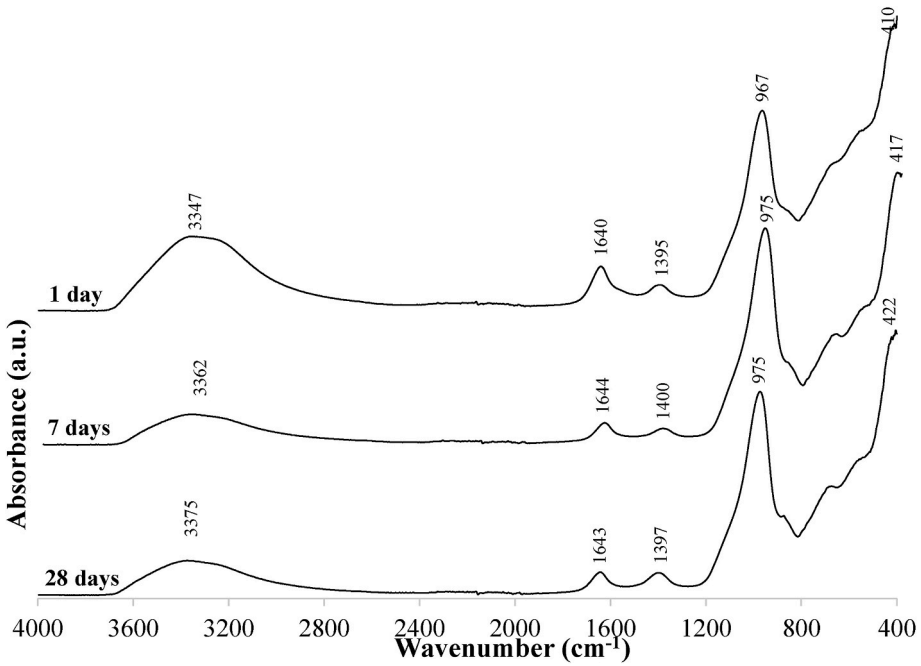

Fig. 8. FTIR spectra of 50MK-50FA blended geopolymers as function of curing time.

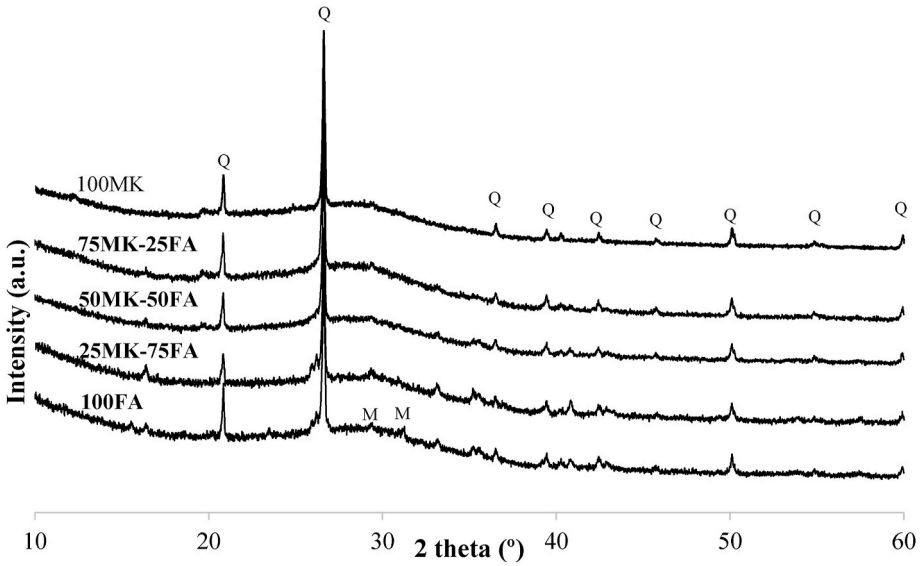

Fig. 9. XRD diffractograms of MK, FA and MK-FA blended geopolymers at 7 days of curing. Q: quartz, M: mullite.

the 100 MK and 100FA geopolymers. However, the thermal conductivity values obtained for the 100MK control geopolymers are similar to those obtained by Kamseu et al. (2012) who synthesized five compositions of MK geopolymers with Si/Al from 1.23 to 2.42 obtaining MK geopolymers with thermal conductivity of 0.30–0.59 W/m K. While the thermal conductivity values obtained for the 100FA geopolymers are lower than the ones obtained by Agustini et al. (2020), which obtained geopolymers with a solids ratio ranging from 0.16 to 0.31 obtaining thermal conductivity values ranging from 0.75 to 1.54 W/m K, but similar to those obtained by Baran et al. (2021) with thermal conductivity values of 0.431 W/mK. The specimens present lower thermal conductivity than of the concretes which could be close to 0.72 W/(m•K) for concrete containing calcium aggregates, or even have values of 1.4–1.6 W/(m•K), depending on the porosity of the concrete (Zhang et al., 2020).

Pearson's correlation coefficient (Table 3) was used to determine the correlation between thermal conductivity and bulk density, compressive strength, apparent porosity and water absorption. This coefficient is used as a measure of the degree of relationship

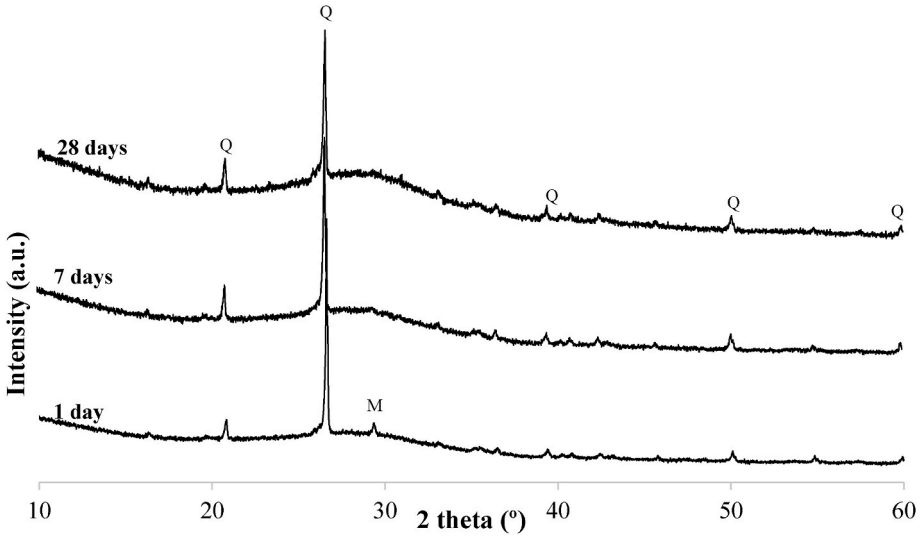

Fig. 10. XRD diffractograms of 50MK-50FA blended geopolymers as function of curing time. Q: quartz, M: mullite.

between two variables. When a Pearson's coefficient closer to a value of 1.0 or −1.0 is obtained, it indicates a stronger direct or inverse correlation, respectively, between the two variables. Thermal conductivity has a strong direct relationship with bulk density and compressive strength, while it has a moderate inverse correlation with bulk porosity and water absorption.

3.4. Functional group analysis

Fig. 6 shows the FTIR spectra of raw materials: MK and FA. MK and FA show a main band centered at 1058 cm^{-1} in the MK precursor and at 1114 and 974 cm^{-1} in the FA residue assigned to the asymmetric stretching vibration of Si–O–Si(Al).

The FTIR spectra of geopolymers after 7 days of curing are shown in Fig. 7. A shift of this band towards lower wavenumbers can be observed due to alkaline activation moving up to 974 cm^{-1} for the MK geopolymers and up to 975-979 cm^{-1} for the MK-FA and FA geopolymers. This band is the fingerprint of the geopolymerization process. The shift of this band indicates the presence of Al(IV) in the aluminosilicate structure formed, indicating that the glassy phases of the MK and FA precursors react with alkali silicates to form new products, sodium aluminosilicate hydrate gel (N-A-S-H) in all geopolymers. The formation of sodium (calcium) aluminosilicato hydrate gel ((N,C)-A-S-H) in FA y MK-FA blended geopolymers can be associated with a broadening in the band centered at 972-979 cm^{-1} (Lee et al., 2014), suggesting the presence of calcium in the gels (Somna et al., 2011). The shift to a lower wavelength as the FA content decreases is due to the mode of vibration of the Al–O bond, which vibrates at lower frequencies than the Si–O bond, or indicates a lower inclusion of Al in its structure (Sun Wei and Zongjin, 2009). Bands centered between 3362 and 3386 cm^{-1} and bands centered at 1644 cm^{-1} due to the existence of water molecules are also observed in the geopolymers. The broad band at higher wavenumbers is attributed to O–H stretching bands due to free or physically bound water molecules on the surface or pores of the gel, while the band centered at 1644 cm^{-1} assigned to H–O–H bending vibration bands is due to the physical presence of free water molecules (Ye et al., 2018). Weak absorption bands of carbonates appear at 1394-1410 cm^{-1} and 873 cm^{-1} due to the carbonation of the geopolymers with the formation of Na_2–CO_3H_2O (Álvarez-Ayuso et al., 2008). The band located at 671 cm^{-1} could be assigned to the vibration mode of the Al–O bond (Allali et al., 2016) and the bands at 409-424 cm^{-1} suggest Si–O/Al–O and Si–O–Al bending vibrations (Hu, 2019).

The influence of curing time was observed by comparing 50MK-50FA blended geopolymers at 1, 7 y 28 days of curing (Fig. 8). It can be observed that after 1 day of curing, the geopolymerization reaction has occurred. A shift of the band centered at 967 cm^{-1} after 1 day of curing to 975 cm^{-1} after 7 and 28 days of curing is observed, indicating a higher dissolution of the precursors at shorter curing times and a higher substitution of SiO_4 tetrahedrons for tetrahedrons of AlO_4 in the geopolymeric gel resulting in lower wavelengths. (Rüscher et al., 2010). Therefore, after 7 days of curing it was observed that the reaction hardly changed, which indicated that for 7 days of curing the geopolymerization process had concluded. The bands assigned to the presence of water, bands centered at 3347-3375 cm^{-1} and 1640-1644 cm^{-1} decrease with increasing curing time from 1 to 7 days and to a lesser extent from 7 to 28 days suggesting that the Si–OH chemical bond increases due to the increase of MK and FA particles available for geopolymer formation (Hu, 2019), as well as the increase of the H–O–H bond size fraction, which causes the band centered at 1640-1644 cm^{-1} to decrease indicating the formation of water molecules as a product of the hydration of the geopolymerization process (Alehyen et al., 2017).

3.5. Phase transformation

Fig. 9 shows XRD difractograms of MK, FA and MK-FA blended geopolymers after 7 days of curing. It can be observed in all geopolymers the presence of a halo at 2 theta 25-35° indicating the formation of N-A-S-H geopolymeric gel and (N,C)-A-S-H gel produced by alkaline reaction of the precursors (Ahmari et al., 2012; Barbosa et al., 2000; Chakouté et al., 2016). The geopolymerization process involves three stages: (1) dissolution of the alumina and silicates initially contained in the precursors (metakaolin and fly ash) in the alkaline solution (2) formation of oligomeric species (the precursors of the geopolymers) consisting of

Table 3
Pearson coefficient of thermal conductivity versus, bulk density, compressive strength apparent porosity and water absorption.

	Pearson Coefficient
Conductivity versus bulk density	0.98
Conductivity versus compressive strength	0.90
Conductivity versus apparent porosity	−0.42
Conductivity versus water absorption	−0.39

Si–O–Si and/or Si–O–Al polymeric bonds and (3) polycondensation of the oligomers to form an aluminosilicate network (Rees et al., 2008). This halo is similar although slightly less intense when FA is incorporated which could indicate that the amount of geopolymer gel formed is almost the same or slightly lower in FA and MK-FA blended geopolymers. These data indicate that large amounts of FA (up to 50 wt%) or FA alone can be employed as precursors in the synthesis of geopolymers having losses in compressive strength of 33.8 and 8.3% respectively. Comparing the diffraction patterns with those of the raw materials, it can be observed the existence of diffraction peaks of quartz, indicating that this crystalline phase is chemically inert in the geopolymerization process (Zhang et al., 2004). In addition, small diffraction peaks corresponding to mullite, the main crystalline phase of fly ash, have been detected. The formation of new crystalline phases was not observed.

Fig. 10 shows the diffractogram of the 50MK-50FA blended geopolymers at 1, 7 and 28 days of curing. It can be observed that the diffractograms do not change with the curing time, indicating that the dissolution of the amorphous phases takes place in the first 24 h when curing at 60 °C and the attack of the alkaline solution to the crystalline phases does not occur after this period of time, increasing in very little proportion the amount of geopolymer gel formed with the curing time and producing fundamentally water evaporation.

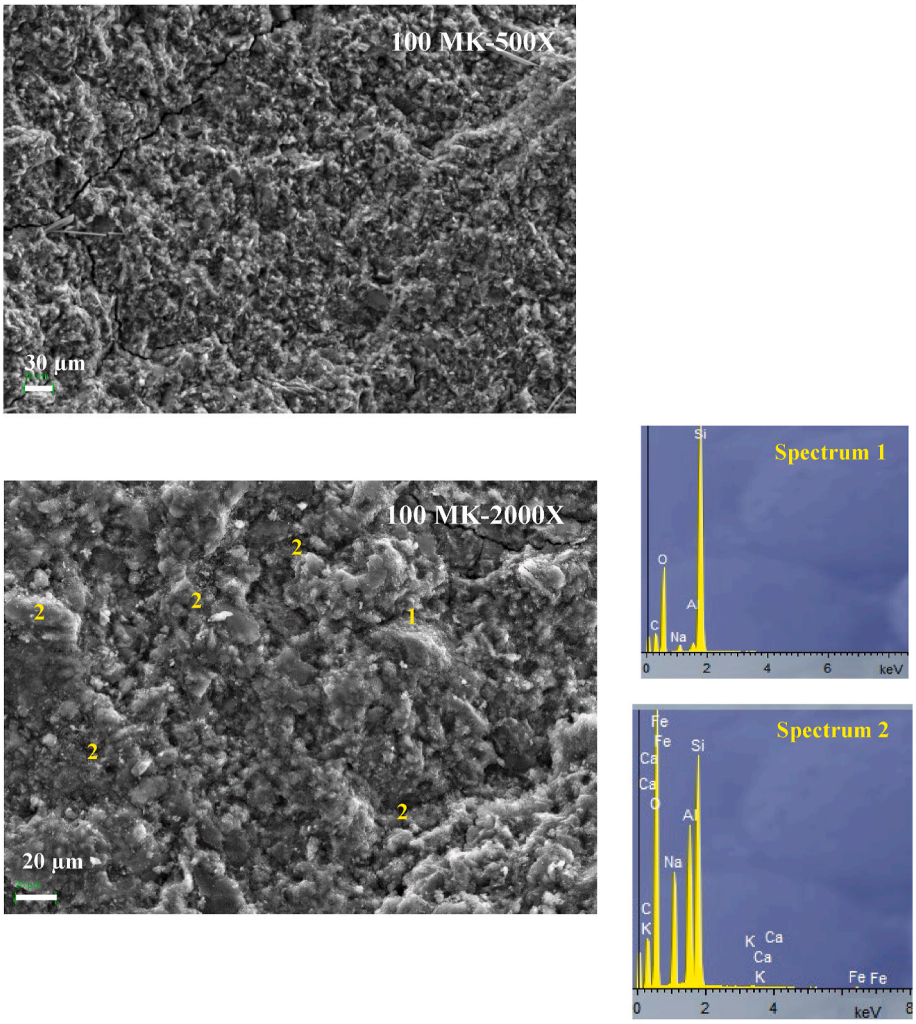

Fig. 11. SEM images and EDS analysis of MK, MK-FA and FA geopolymers at two magnifications 500X and 2000X after 7 days of curing.

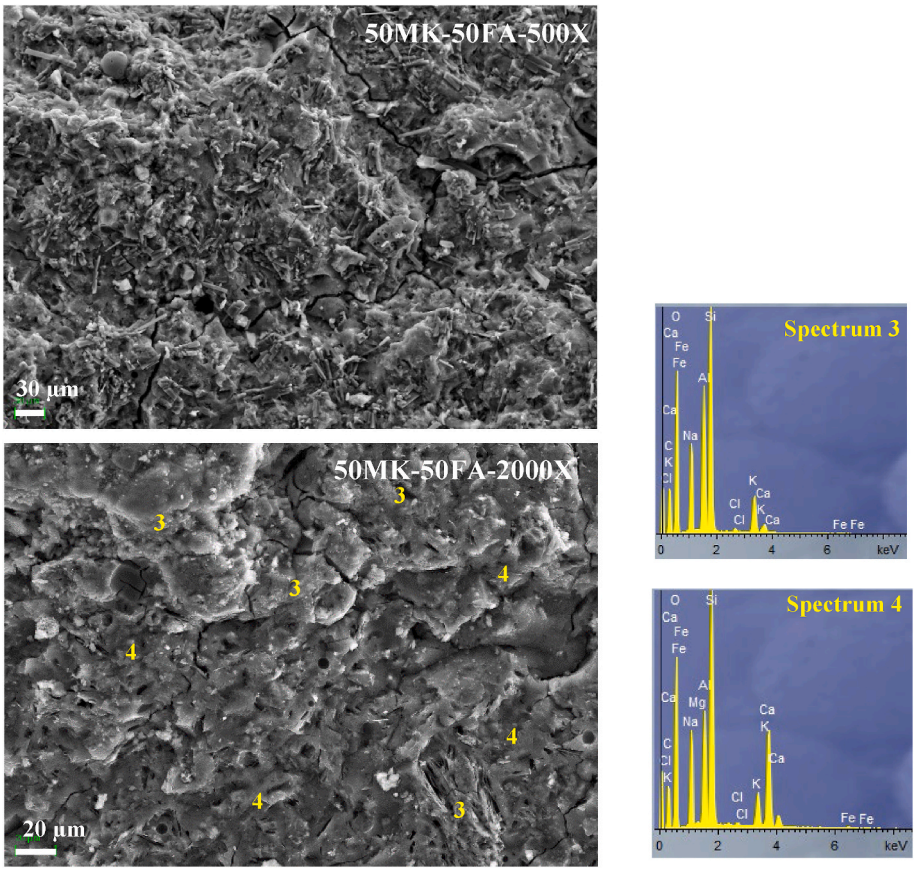

Fig. 11. (*continued*).

3.6. Microstructural analysis

Micromorphology observations de 100MK, 100FA and 50MK-50FA blended geopolymers were obtained by SEM at 500 X and 2000 X and the chemical composition was analyzed using Energy Dispersive X-rays spectroscopy (EDS) (Fig. 11). It can be observed how the pure metakaolin based geopolymer presents a less dense structure, where there is a very small proportion of unreacted MK particles (Spectrum 1), microcracks and pores, with a higher proportion of N-A-S-H gel (Spectrum 2) (Longhi et al., 2020; Živica and Palou, 2016). The FA geopolymers present a denser structure with the existence of unreacted ash spheres or particles (Spectrum 5) and the presence of microcracks, as well as the formation of (C, N)-A-S-H gel (Spectrum 6) due to the presence of calcium in the FA possibly due to its carbonation. The MK-FA blended geopolymers present regions with N-A-S-H with similar appearance to the gel formed in the MK geopolymers, richer in sodium (Spectrum 3) and gel similar to that formed in the FA geopolymers, richer in calcium (Spectrum 4), as well as microcracks. The microcracks are formed by water evaporation and shrinkage during thermal curing.

4. Conclusions

Metakaolin, coal fly ash and metakaolin and coal fly ash with different weight ratios (25–75; 50-50 and 75-25) were used as a source of aluminosilicates for the synthesis of geopolymers. The results indicate that bulk density increases and apparent porosity and water absorption decrease as increasing amounts of FA are incorporated at 7 days of curing. However, at 28 days of curing, the opposite occurs: bulk density decreases and bulk porosity and water absorption increase with FA content, due to the higher water evaporation in these samples due to the excess of free water in the geopolymers as the FA content increases, due to the higher workability of the FA residue due to the spherical shape of the particles which may require lower s/l ratios. The compressive strength and thermal conductivity of the blended geopolymers are slightly lower than those using only MK or only FA as precursors. The compressive strength increases as the Si/Al ratio decreases, and the Na/Al ratio except for FA geopolymers. The excess of water in FA and MK-FA blended geopolymers may be responsible for the poorer mechanical properties of these specimens with respect to MK geopolymers despite the presence of (C,N)-A-S-H gel. Bulk density and compressive strength have a significant effect on the thermal conductivity of specimens. The XRD FTIR and SEM analysis confirm the formation of the N-A-S-H geopolymeric gel for MK geopolymers, (C,N)-A-S-H gel in FA geopolymers and N-A-S-H and (N,C)-A-S-H gel in the MK-FA blended geopolymers at 1, 7 and 28 days of curing, being higher the amount of aluminosilicate gel with respect to silicate gel in geopolymers with lower Si/Al ratio. The results indicate that the use of FA residue and the substitution of FA by MK in the synthesis of geopolymers can be a satisfactory solution for the recovery of waste,

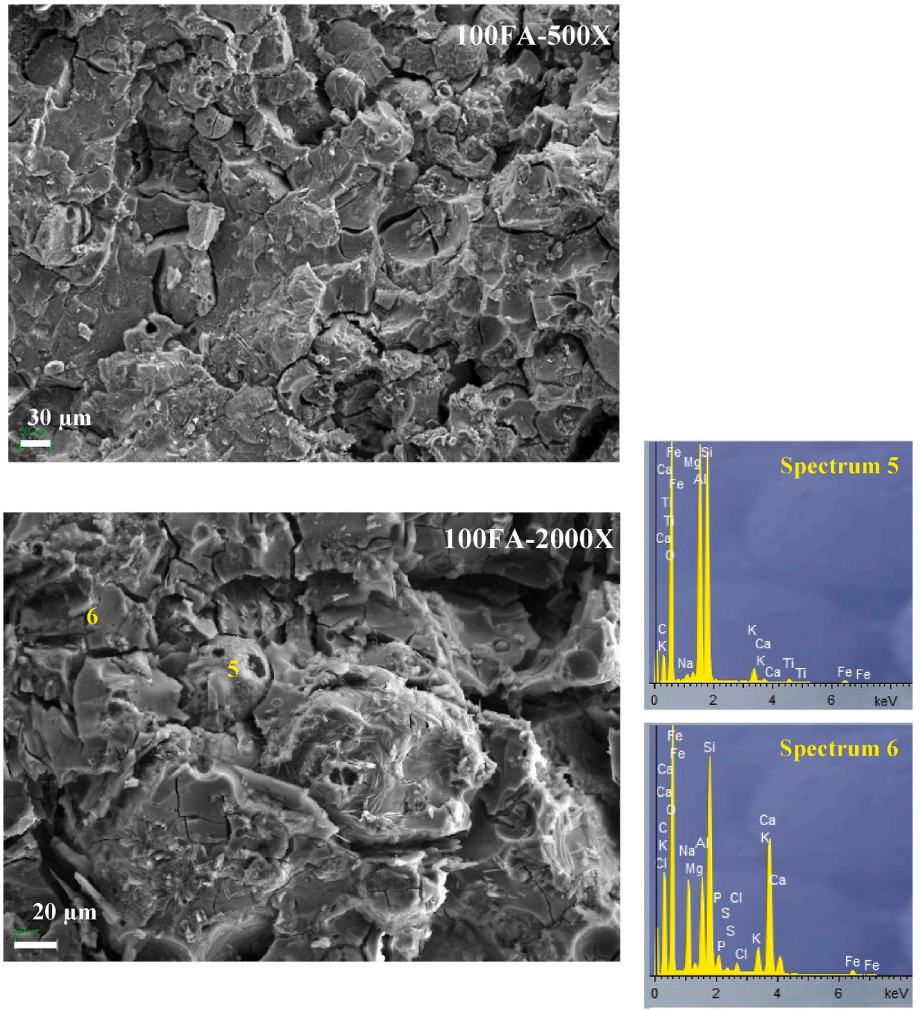

Fig. 11. (*continued*).

approaching the principles of the circular economy, obtaining sustainable construction materials that can be used for loadbering concrete masonry units with insulating properties far superior to those of Portland Cement conventionals. However, it is necessary to optimize the s/l ratio of FA and MK-FA blended geopolymers in order to improve the physical and mechanical properties of these geopolymers.

Author contribution

M.A. Gómez-Casero: investigation, manufactures some geopolymers and performs some test, data curation, C. De Dios-Arana: investigation, manufactures the geopolymer and performs the tests; data curation; L. Pérez-Villarejo: writing - review & editing. S. Bueno-Rodríguez: writing - review & editing. D. Eliche-Quesada: conceptualization.; formal analysis, investigation; resources; data curation; writing - original draft; writing-review & editing; visualization; supervision; project administration and funding acquisition.

Declaration of competing interest

The authors declare that they have no known competing financial interests or personal relationships that could have appeared to influence the work reported in this paper.

Acknowledgements

This work has been funded by the project *Development and characterization of new geopolymeric composites based on waste from the olive industry. Towards a sustainable construction* (MAT2017-88097-R), FEDER/Ministry of Science, Innovation and Universities, State Research Agency. M.A. Gómez-Casero acknowledges support of MINECO (PRE2018-084073). The authors thank "Caobar S.A." company and "Central térmica Litoral de Almería" for supplying the kaolinite and coal fly ash, respectively. Technical and human

support provided by CICT of Universidad de Jaén (UJA, MINECO, Junta de Andalucía, FEDER) is gratefully acknowledged.

References

Abdullah, S., Ming, L.Y., Abdullah, M.M.A., Yong, H.C., Zulkifly, K., 2018. Evaluation on mixing parameter of S/L and Na2SiO3/NaOH ratios towards fly ash geopolymers. In: AIP Conference Proceedings 2030. AIP Publishing LLC, 020295. https://doi.org/10.1063/1.5066936.

Adesanya, E., Ohenoja, K., Di Maria, A., Kinnunen, P., Illikainen, M., 2020. Alternative alkali-activator from Steel-making Waste for one-part alkali-activated slag. J. Clean. Prod. 274, 123020. https://doi.org/10.1016/j.jclepro.2020.1230.

Aguilar, R.A., Díaz, O.B., García, J.E., 2010. Lightweight concretes of activated metakaolin-fly ash binders, with blast furnace slag aggregates. Construct. Build. Mater. 24 (7), 1166–1175. https://doi.org/10.1016/j.conbuildmat.2009.12.024.

Agustini, N.K.A., Triwiyono, A., Sulistyo, Suyitno, D., 2020. Effects of water to solid ratio on thermal conductivity of fly ash-based geopolymer paste. IOP Conf. Ser. Earth Environ. Sci. 426, 012010 https://doi.org/10.1088/1755-1315/426/1/012010.

Ahmari, S., Ren, X., Toufigh, V., Zhang, L., 2012. Production of geopolymeric binder from blended waste concrete powder and fly ash. Construct. Build. Mater. 35, 718–729. https://doi.org/10.1016/j.conbuildmat.2012.04.044, 2012.

Alehyen, S., Achouri, M.E.L., Taibi, M., 2017. Characterization , microstructure and properties of fly ash-based geopolymer. J. Mater. Environ. Sci. 8, 1783–1796. https://doi.org/10.1165/2014/172753.49.

Allali, F., Joussein, E., Kandri, N.I., Rossignol, S., 2016. The influence of calcium content on the mixture of sodium silicate with different additives: Na_2CO_3, NaOH and AlO(OH). Construct. Build. Mater. 121, 588–598. https://doi.org/10.1016/j.conbuildmat.2016.06.034.

Álvarez-Ayuso, E., Querola, Q., Plana, F., Alastuey, A., Moreno, N., Izquierdo, M., Fonta, O., Moreno, T., Diez, S., Vázquez, E., Barra, M., 2008. Environmental, physical and structural characterisation of geopolymer matrixes synthesised from coal (co-)combustion fly ashes. Hazard. Mater. 154 (1–3), 175–183. https://doi.org/10.1016/j.jhazmat.2007.10.008.

Arun, B.R., Nagaraja, P.S., Srishaila, J.M., 2019. An effect of NaOH molarity on fly ash—metakaolin-based self-compacting geopolymer concrete. In: Das, B., Neithalath, N. (Eds.), Sustainable Construction and Building Materials, Lecture Notes in Civil Engineering, vol. 25. Springer, Singapore. https://doi.org/10.1007/978-981-13-3317-0_21.

ASTM C618, 2003. Standard specification for coal fly ash and raw or calcined natural pozzolan for use in concrete. In: American Society for Testing and Materials. ASTM international, West Conshohocken, PA, USA. www.astm.org.

ASTM C642-13, 2013. Standard test method for density, absorption, and voids in hardened concrete, ASTM international, west conshohocken, PA. www.astm.org.

ASTM C90-16a, 2016. Standard specification for loadbearing concrete masonry units, ASTM international, west conshohocken, PA. www.astm.org.

Baran, P., Nazarkoc, M., Włosińska, E., Kanciruk, A., Zarębska, K., 2021. Synthesis of geopolymers derived from fly ash with an addition of perlite. J. Clean. Prod. 293, 126112. https://doi.org/10.1016/j.jclepro.2021.126112.

Barbosa, V.F., MacKenzie, K.J., Thaumaturgo, C., 2000. Synthesis and characterisation of materials based on inorganic polymers of alumina and silica: sodium polysialate polymers. Int. J. Inorg. Mater. 2 (4), 309–317. https://doi.org/10.1016/S1466-6049(00)00041-6, 2000.

Bidwe, S.S., Hamane, A.A., 2015. Effect of different molarities of sodium hydroxide solution on the strength of geopolymer concrete. Am. Eng. Res. 4 (3), 2320-0847.

Bing-hui, M., Zhu, H., Xue-min, C., Yan, H., Si-yu, G., 2014. Effect of curing temperature on geopolymerization of metakaolin-based geopolymers. Appl. Clay Sci. 99, 144–148. https://doi.org/10.1016/j.clay.2014.06.024.

Cai, J., Li, X., Tan, J., Vandevyvere, B., 2020. Thermal and compressive behaviors of fly ash and metakaolin-based geopolymer. J. Build. Eng. 30, 101307. https://doi.org/10.1016/j.jobe.2020.101307.

Cavusoglu, I., Yilmaz, E., Yilmaz, A.O., 2021. Sodium silicate effect on setting properties, strength behaviour and microstructure of cemented coal fly ash backfill. Construct. Build. Mater. 267, 121021. https://doi.org/10.1016/j.powtec.2021.02.013.

Chakouté, H.K.T., Rüscher, C.H., Kong, S., Kamseu, E., Leonelli, C., 2016. Geopolymer binders from metakaolin using sodium waterglass from waste glass and rice husk ash as alternative activators: a comparative study. Construct. Build. Mater. 114, 276–289. https://doi.org/10.1016/j.conbuildmat.2016.03.184.

Chen, Y., Zhou, X., Wan, S., Zhen, R., Tong, J., Hou, H., Wang, T., 2019. Synthesis and characterization of geopolymers composites based on gasification coal fly ash and steel slag. Construct. Build. Mater. 211, 646–658. https://doi.org/10.1016/j.conbuildmat.2019.03.292.

Cheng-Yong, H., Yun-Ming, L., Abdullah, M.M.A.B., Hussin, K., 2017. Thermal resistance variations of fly ash geopolymers: foaming responses. Sci. Rep. 7 (1), 1–11. https://doi.org/10.1038/srep45355.

ECOBA, 2021. European association for use of the by-products of coal-fired power stations. http://www.ecoba.com.

Elavarasan, S., Priya, A.K., Kumar, V.K., 2021. Manufacturing fired clay brick using fly ash and M-sand. Mater. Today Proc. 37, 872–876. https://doi.org/10.1016/j.matpr.2020.06.042.

Eléctrica de España, Red, 2017. Spanish Electrical System. Avance 2016., Madrid.

Eliche-Quesada, D., Sandalio-Pérez, J.A., Martínez-Martínez, S., Pérez-Villarejo, L., Sánchez-Soto, P.J., 2018. Investigation of use of coal fly ash in eco-friendly construction materials: fired clay bricks and silica-calcareous non fired bricks. Ceram. Int. 44, 4400–4412. https://doi.org/10.1016/j.ceramint.2017.12.039.

Fan, Z., Gesser, H.D., 1996. Recovery of gallium from coal fly ash. Hydrometallurgy 41, 187–200.

Fawer, M., Concannon, M., Rieber, W., 1999. Life cycle inventories for the production of sodium silicates. Int. J. Life Cycle Assess. 4 (4), 201–212. https://doi.org/10.1007/BF02979498.

Feng, J., Zhang, R., Gong, L., Li, Y., Cao, W., Cheng, X., 2015. Development of porous fly ash-based geopolymer with low thermal conductivity. Mater. Des. 65, 529–533. https://doi.org/10.1016/j.matdes.2014.09.024.

Fernández-Jiménez, A., Palomo, A., Sobrados, I., Sanz, J., 2006. The role played by the reactive alumina content in the alkaline activation of fly ashes. Microporous Mesoporous Mater. 91 (1–3), 111–119. https://doi.org/10.1016/j.micromeso.2005.11.015.

Fongang, R.T.T., Pemndje, J., Lemougna, P.N., Chinje Melo, U., Nanseua, C.P., Nait-Ali, B., Kamseu, E., Leonelli, C., 2015. Cleaner production of the lightweight insulating composites: microstructure, pore network and thermal conductivity. Energy Build. 107, 113–122. https://doi.org/10.1016/j.enbuild.2015.08.009.

Font, O., Querol, X., Lopez-Soler, A., Chimenos, J.M., Fernandez, A.I., Burgos, S., Garcia, P.F., 2005. Ge extraction from gasification fly ash. Fuel 84, 1384–1392. https://doi.org/10.1016/j.fuel.2004.06.041.

Gingos, G.S., 2011. Effect of PFA on strength and water absorption of mortar. J. Civ. Eng. Sci. Technol. 2, 7–11. https://doi.org/10.33736/jcest.81.2011.

Gómez-Casero, M.A., Pérez-Villarejo, L., Castro, E., Eliche-Quesada, D., 2021. Effect of steel slag and curing temperature on the improvement in technological properties of biomass bottom ash based alkali-activated materials. Construct. Build. Mater. 302, 124205. https://doi.org/10.1016/j.conbuildmat.2021.124205.

Guo, H., Yuan, P., Zhang, B., Wang, Q., Deng, L., Liu, D., 2021. Realization of high-percentage addition of fly ash in the materials for the preparation of geopolymer derived from acid-activated metakaolin. J. Clean. Prod. 285, 125430. https://doi.org/10.1016/j.jclepro.2020.125430.

He, Y., Cheng, W.M., Cai, H.S., 2005. Characterization of α-cordierite glass-ceramics from fly ash. J. Hazard Mater. 120, 265–269. https://doi.org/10.1016/j.jhazmat.2004.10.028Get.

He, J., Yu, J., Zhang, Y., Zhang, G., 2012. The strength and microstructure of two geopolymers derived from metakaolin and red mud-fly ash admixture: a comparative study. Construct. Build. Mater. 30, 80–91. https://doi.org/10.1016/j.conbuildmat.2011.12.011.

Hu, Y., 2019. Role of Fe species in geopolymer synthesized from alkali-thermal pretreated Fe-rich Bayer red mud. Construct. Build. Mater. 200, 398–407. https://doi.org/10.1016/j.conbuildmat.2018.12.12.

Jaya, N.A., Yun-Ming, L., Cheng-Yon, H., Mustafa Al Bakri, M., Kamarudin Hussin, A., 2020. Correlation between pore structure, compressive strength and thermal conductivity of porous metakaolin geopolymer. Construct. Build. Mater. 247, 118641. https://doi.org/10.1016/j.conbuildmat.2020.118641.

Kamseu, E., Ceron, B., Tobias, H., et al., 2012. Insulating behavior of metakaolin-based geopolymer materials assess with heat flux meter and laser flash techniques. J. Therm. Anal. Calorim. 108, 1189–1199. https://doi.org/10.1007/s10973-011-1798-9.

Koshy, N., Dondrob, K., Hu, L., Wen, Q., Meegoda, J.N., 2019. Synthesis and characterization of geopolymers derived from coal gangue, fly ash and red mud. Construct. Build. Mater. 206, 287–296.

Lee, J.K., Shang, J.Q., Wang, H., Zhao, C., 2014. In situ study of beneficial utilization of coal fly ash in reactive mine tailings. J. Environ. Manag. 135, 73–80. https://doi.org/10.1016/j.jenvman.2014.01.012.
Li, C., Sun, H., Li, L., 2010. A review: the comparison between alkali-activated slag (Si + Ca) and metakaolin (Si + Al) cements. Cement Concr. Res. 40, 1341–1349. https://doi.org/10.1016/j.cemconres.2010.03.020.
Longhi, E.D., Rodríguez, B., Walkley, Z., Zhang, A.P. Kirchheim, 2020. Metakaolin-based geopolymers: relation between formulation, physicochemical properties and efflorescence formation. Compos. Part. B. 182, 107671. https://doi.org/10.1016/j.compositesb.2019.107671.
Novais, R.M., Buruberri, L.H., Ascensao, G., Seabra, M.P., Labrincha, J.A., 2016. Porous biomass fly ash-based geopolymers with tailored thermal conductivity. J. Clean. Prod. 119, 99–107. https://doi.org/10.1016/j.jclepro.2016.01.083.
Ozer, I., Soyer-Uzun, S., 2015. Relations between the structural characteristics and compressive strength in metakaolin based geopolymers with different molar Si/Al ratios. Ceram. Int. 41, 10192–10198. https://doi.org/10.1016/j.ceramint.2015.04.125.
Pandey, V.C., Singh, N., 2010. Impact of fly ash incorporation in soil systems. Agric. Ecosyst. Environ. 136, 16–27. https://doi.org/10.1016/j.agee.2009.11.013.
Qin, L., Gao, X., Li, Q., 2019. Influences of coal fly ash containing ammonium salts on properties of cement paste. J. Environ. Manag. 249, 109374. https://doi.org/10.1016/j.jenvman.2019.109374.
Querol, X., Moreno, N., Umaña, J.C., Alastuey, A., Hernández, E., López-Soler, A., plana, F., 2002. Synthesis of seolite from coal fly ash: an overview. Int. J. Coal Geol. 5, 413–423. https://doi.org/10.1016/S0166-5162(02)00124-6.
Rees, C., Provis, J.L., Lukey, G., Deventer, J., 2008. The mechanism of geopolymer gel formation investigated thought seeded nucleation. Colloids Surf. A Physicochem. Eng. Asp. 318, 97–105. https://doi.org/10.1016/j.colsurfa.2007.12.019.
Rovnaník, P., 2010. Effect of curing temperature on the development of hard structure of metakaolin-based geopolymer. Construct. Build. Mater. 24 (7), 1176–1183. https://doi.org/10.1016/j.conbuildmat.2009.12.023.
Rüscher, C.H., Mielcarek, E., Lutz, W., Ritzmann, A., Kriven, W.M., 2010. Weakening of alkali-activated metakaolin during aging investigated by the molybdate method and infrared absorption spectroscopy. J. Am. Ceram. Soc. 93, 2585–2590. https://doi.org/10.1111/j.1551-2916.2010.03773.x.
Sajan, P., Jiang, T., Lau Ch, Ch, Tan, G., Ng, K., 2021. Combined effect of curing temperature, curing period and alkaline concentration on the mechanical properties of fly ash-based geopolymer. Clean. Mater. 1, 100002. https://doi.org/10.1016/j.clema.2021.100002.
Shi, Y., Jiang, K.X., Zhang, T.A., 2020. A cleaner electrolysis process to recover alumina from synthetic sulphuric acid leachate of coal fly ash. Hydrometallurgy 191, 105196. https://doi.org/10.1016/j.hydromet.2019.105196.
Sisol, M., Kudelas, D., Marcin, M., Holub, T., Varga, P., 2019. Statistical evaluation of mechanical properties of slag based alkali-activated material. Sustainability 11 (21), 5935. https://doi.org/10.3390/su11215935.
Sokolar, R., Vodova, L., 2011. The effect of fluidized fly ash on the properties of dry pressed ceramic tiles based on fly ash–clay body. Ceram. Int. 37 (7), 2879–2885. https://doi.org/10.1016/j.ceramint.2011.05.005.
Somna, K., Jaturapitakkul, Ch, Kajitvichyanukul, P., Chindaprasirt, P., 2011. NaOH-activated ground fly ash geopolymer cured at ambient temperature. Fuel 90, 2118–2124. https://doi.org/10.1016/j.fuel.2011.01.018.
Sun Wei, Z.Y., Zongjin, L., 2009. Preparation and microstructure of Na-PSDS geopolymeric matrix. Ceram. Silikáty 53, 88–89.
UNE-EN 1015-11:2000/A1:2007, 2007. Methods of Test for Mortar for Masonry – Part 11: Determination of Flexural and Compressive Strength of Hardened Mortar.
Wang, Y., Cao, Y., Zhang, P., Ma, Y., Zhao, T., Wang, H., Zhang, Z., 2019. Water absorption and chloride diffusivity of concrete under the coupling effect of uniaxial compressive load and freeze-thaw cycles. Construct. Build. Mater. 209, 566–576. https://doi.org/10.1016/j.conbuildmat.2019.03.091.
Wang, Y.S., Alrefaei, Y., Dai, J.G., 2020. Influence of coal fly ash on the early performance enhancement and formation mechanism of silico-aluminophosphate geopolymer. Cement Concr. Res. 127, 105932. https://doi.org/10.1016/j.cemconres.2019.105932.
Xu, H., van Deventer, J.S.J., 2003. Effect of source materials on geopolymerization. Ind. Eng. Chem. Res. 42, 1698–1706. https://doi.org/10.1021/ie0206958.
Yang, X., Liu, J., Li, H., Xu, L., Ren, Q., Li, L., 2019. Effect of triethanolamine hydrochloride on ther performance of cement paste. Construct. Build. Mater. 200, 218–225. https://doi.org/10.1016/j.conbuildmat.2018.12.124.
Yao, Z.T., Ji, X.S., Sarker, P.K., Tang, J.H., Ge, L.Q., Xia, M.S., Xi, Y.Q., 2015. A comprehensive review on the applications of coal fly ash. Earth Sci. Rev. 141, 105–121. https://doi.org/10.1016/j.earscirev.2014.11.016.
Ye, H., Zhang, Y., Yu, Z., Mu, J., 2018. Effects of cellulose, hemicellulose, and lignin on the morphology and mechanical properties of metakaolin-based geopolymer. Construct. Build. Mater. 173, 10–16. https://doi.org/10.1016/j.conbuildmat.2018.04.028.
Yun-Minga, L., Cheng-Yong, H., Mustafa Al Bakria, M., Hussin, K., 2016. Structure and properties of clay-based geopolymer cements: a review. Prog. Mater. Sci. 83, 595–629. https://doi.org/10.1016/j.pmatsci.2016.08.002.
Zhang, S., Gong, K., Lu, J., 2004. Novel modification method for inorganic geopolymer by using water soluble organic polymers. Mater. Lett. 58 (7–8), 1292–1296. https://doi.org/10.1016/j.matlet.2003.07.051.
Zhang, S., Zhou, H., Wang, H., 2020. Thermal conductive properties of solid-liquid-gas three-phase unsaturated concrete. Construct. Build. Mater. 232, 117242. https://doi.org/10.1016/j.conbuildmat.2019.117242.
Živica, V., Palou, M., 2016. Influence of heat treatment on the pore structure of some clays-precursors for geopolymer synthesis. Procedia Eng. 151, 141–148. https://doi.org/10.1016/j.proeng.2016.07.401.
Zulkifly, K., Cheng-Yong, H., Yun-Ming, L., Abdullah, M.M.A.B., Shee-Ween, O., Khalid, M.S.B., 2021. Effect of phosphate addition on room-temperature-cured fly ash-metakaolin blend geopolymers. Construct. Build. Mater. 270, 121486. https://doi.org/10.1016/j.conbuildmat.2020.121486.